

Electrical and Mechanical Properties of Twisted Carbon Nanotubes

Alain Rochefort[†] and Phaedon Avouris[‡].

[†] *Centre de recherche en calcul appliqué (CERCA), 5160 boul. Décarie, bureau 400, Montréal, Qc, Canada H3X 2H9.*

[‡] *IBM Research Division, T.J. Watson Research Center, P.O. Box 218, Yorktown Heights, NY 10598, USA.*

We have evaluated the energies required to twist carbon nanotubes (NTs), and investigated the effects of these distortions on their electronic structure and electrical properties. The computed distortion energies are high, indicating that it is unlikely that extensive twisting is the result of thermal excitation. Twisting strongly affects the electronic structure of NTs. Normally metallic armchair (n, n) NTs develop a band-gap which initially scales linearly with twisting angle and then reaches a constant value. This saturation is associated with a structural transition to a flattened helical structure. The values of the twisting energy and of the band-gap are strongly affected by allowing structural relaxation in the twisted structures. Finally, we have used the Landauer-Büttiker formalism to calculate the electrical transport of the metal-NT-metal system as a function of the NT distortion.

Research on the electronic properties of carbon nanotubes (NTs) has been an especially active field in recent years. The reasons for this are twofold: on one hand they are viewed as potential building blocks of nano-sized electronic devices [1–3]. On the other hand, they are ideal materials to study electrical transport phenomena in low-dimensional systems, and to test the theoretical models proposed to explain such phenomena. NTs are usually thought of as a graphene sheet rolled up to form a compact cylinder with a radius that can be as small as a few Angströms [4]. It is obvious, however, that this picture of a NT as a straight, geometrically and atomically perfect tube is somewhat oversimplified. Images of NTs quite often reveal structural deformations such as bent [5], twisted [6], or collapsed [7] tubes. These deformations may develop during growth, deposition and processing, or following an interaction with surface features such as electrodes, or other NTs. An investigation of the electronic structure of weakly distorted nanotubes has been performed using a low energy field theory description [8,9]. Here we aim to study the distortion energies, electronic properties, and electrical transport of carbon nanotubes under a wide range of twisting distortions.

The electronic properties of carbon nanotubes are usually discussed in terms of the π electronic structure of the 2D-graphene sheet. The mapping of the graphene sheet onto a cylindrical surface is specified by a superlattice translational vector $\vec{T} = n\vec{T}_1 + m\vec{T}_2$ where $\vec{T}_1 = a(1, 0)$ and $\vec{T}_2 = a(1/2, \sqrt{3}/2)$, and a is the length of the primitive translation vector of the graphite lattice. The pair of indices (n, m) describes how the NT is wrapped to form the cylinder, and determines its electrical properties. An (n, n) , so called "armchair" tube, has only two linearly

independent Fermi points $\pm\vec{K}$, where $\vec{K} = (k_F, 0)$. It is a metal with two bands intersecting the Fermi energy [10–12]. Thus, when an (n, n) NT is atomically perfect and undistorted, it is expected to exhibit at low bias a quantized conductance equal to $4e^2/h$. However, even in the case of a perfect NT, a reduction of the conductance may be observed due to the non perfect transmission at the NT-metal electrode contacts.

The low energy theory [8,9] used previously to describe the electronic structure of distorted carbon NTs considers only the π -orbitals, and can be appropriately described by a tight-binding model in which deformations are taken into account simply by modifying the hopping amplitudes at the deformation sites. This analysis shows that a smooth bending of the tube along its axis of rotation has little influence on its electronic properties. On the other hand, it predicts that a twisting deformation can lead to substantial modification of the electronic structure. The low energy theory is applicable to small deformations. Large deformations induce the mixing of orbitals, so that describing the electronic structure changes simply by modifying the hopping amplitudes is no longer adequate. In previous work [13], we computed the electronic properties of bent NTs. We found that there is a maximal bending angle above which the low energy theory breaks down and the transport properties are substantially changed. Here we extend this work by studying the effect of twisting distortions over a wide range of twisting angles using a model that takes into account of both the s and p carbon orbitals, as well as allowing the geometrical relaxation of the distorted structures.

The nanotube model used in the computations contains 948 carbon atoms arranged in an armchair (6,6) structure. The energetics of the deformations were determined with molecular mechanics using the TINKER program [14] with a modified MM3 force-field [15]. Calculations were also performed using a tight-binding density functional theory (TB-DFT) method developed by Porezag *et al.* [16]. In both types of calculations the dangling bonds at the ends of the tubes were saturated by hydrogen atoms. Distorted structures were generated by two different schemes. In the first, continuous twisting, the circular plane sections of carbon atoms along the tube axis were rotated sequentially by an (additive) specified angle. In the second, alternate twisting, a (non-additive) rotation was performed on every second section. The molecular mechanics calculations showed that it is less energetically demanding to continuously twist the tube than to twist it alternatively. Therefore, in the rest of the

paper, we will focus our attention on continuous deformations. The electronic structures of twisted NTs were determined using the extended Hückel method (EHM) [17]. EHM gives results similar to those obtained on extended NTs with more sophisticated methods [18]. The energy band-gap was obtained as the difference between the HOMO and LUMO energies.

To evaluate the transport properties, the two ends (with dangling bonds) of the NT were bonded to gold electrodes. The computation of the transmission function was then carried out by using the Landauer-Büttiker formalism as described in detail in ref. [19]. In this scheme, the retarded Green's function for the system is given by:

$$G^R = \frac{1}{ES_{NT} - H_{NT} - \Sigma_1 - \Sigma_2} \quad (1)$$

where H_{NT} and S_{NT} are the Hamiltonian and the overlap matrices for the carbon nanotube, and $\Sigma_{1,2}$ are self-energies describing the interaction of the NT with the metal contacts. These are given by:

$$\Sigma_j = \tau_j^\dagger g_j \tau_j \quad (2)$$

with τ_j describing the coupling between the NT and contact j and g_j the Green's function of the metal used for the contacts. The total transmission function from one contact to the other is then given by:

$$T(E) = \text{Tr}[\Gamma_2 G \Gamma_1 G^\dagger] \quad (3)$$

with $\Gamma_j = i(\Sigma_j - \Sigma_j^\dagger)$.

In Figure 1, we plot the potential energy for a continuous twisting deformation against the twist angle for a constrained (6,6) structure, and for a relaxed one where only the first two carbon sections at each end of the tube were held fixed. In the inset, we compare the energies obtained with molecular mechanics for small angle twisting of the relaxed structures to the energies determined with the TB-DFT method. A number of observations can be made. First, the energy required for even a moderate twisting of the tube is very large. At low twisting angles (inset) a quadratic law is obeyed. The twisting energies calculated using the MM3 potentials are lower than those computed using TB-DFT (inset). Therefore, in the following we will consider the MM3 energies as lower limits to the energetics of twisting deformations. Figure 1 shows clearly that structural relaxation has a very strong effect on the potential energy of deformation, especially for large twisting angles where the relaxation energy is computed to be of about the same order of magnitude as the final energy. Furthermore, the energy profile of the relaxed structure deviates from the quadratic law (dot-dashed line) for $\Theta_T > 14^\circ\text{nm}^{-1}$. This deviation corresponds to the onset of a structural transformation where the tube flattens and takes on a helical shape (such as in Figure 2 [c,d]). A similar transition has been observed in molecular dynamics simulations [20]. In order

to determine the effect of the diameter on the collapsing of the nanotubular structures, we have also computed MM3 energies of twisted (10,10) models. Taking into account the differences in the number of carbon atoms involved $((10,10)/(6,6) = 1.67)$, and the NT diameters $(\phi_{(10,10)}/\phi_{(6,6)} = 1.67)$, we find that the energy needed to twist a (10,10) NT is similar to that needed to twist a (6,6) NT. The collapse of the (10,10) tubular structure into the helical shape occurs at a lower twisting angle than the (6,6) structure, i.e. when $\Theta_T > 10^\circ\text{nm}^{-1}$. However, due to its larger diameter, the relative displacement of the carbon atoms during the tube to helix transition for a (10,10) NT is larger than in the case of a (6,6) NT.

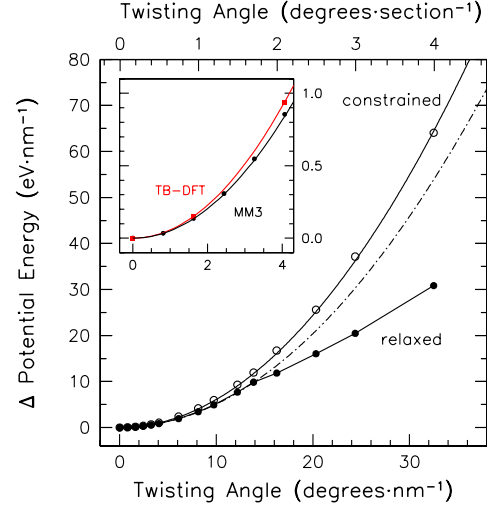


FIG. 1. Molecular mechanics calculation of the energy required to twist a (6,6) armchair NT as a function of twist angle, for a constrained (open circles) and a relaxed geometry (closed circles). The dot-dashed line corresponds to the quadratic law determined from the low twisting angle region of the relaxed NT. The inset shows a comparison of the MM3 and TB-DFT energies for small twisting angle.

Our calculations also showed that the twisting energies scale nearly linearly with the length of the nanotube. Therefore, we can extrapolate and obtain the twisting energies of longer nanotube segments, and use these energies to evaluate their Boltzmann distributions as a function of temperature. The relative population of twisted (6,6) structures can be described by:

$$F(\Theta_T) = \exp\left[-\alpha \cdot \frac{L\Theta_T^2}{T}\right] \quad (4)$$

where, α is a constant equal to $580 \text{ nm}\cdot\text{degree}^{-2}\cdot\text{K}$, L is the nanotube length in nm, Θ_T is the twisting angle ($\text{degree}\cdot\text{nm}^{-1}$), and T is the temperature. From this equation, it is clear that large twists cannot be generated by thermal excitation. For example, to obtain by thermal excitation a relatively small population (1%) of a $1 \mu\text{m}$ long (6,6) nanotube twisted by 9.8°nm^{-1} , which is equivalent to the twist deformation obtained by Clauss

et al. from STM images of nanotube ropes [6], it would require a temperature larger than 10^6 K! We conclude then that large scale nanotube twists must be the result of either mechanical interactions taking place during the deposition or manipulation of the nanotube sample, or they are introduced during the high energy growth processes and frozen in place by shear forces due to the interaction with the substrate and other tubes. Local twisting associated with tube collapse is, however, less energetically demanding and is encountered quite often in AFM images.

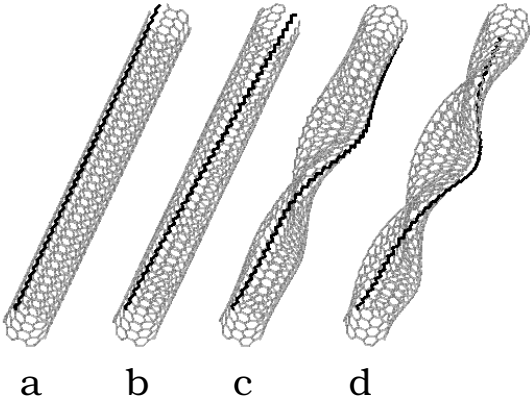


FIG. 2. Relaxed NT structures obtained with force-field MM3 energy minimization on 0 (a), 1 (b), 2 (c) and $3^\circ/\text{section}^{-1}$ (d) twisted models.

We now consider the electronic structure changes induced by twisting the NTs. Figure 3 shows the variation of the band-gap value of a twisted (6,6) nanotube as a function of the twisting angle, for both constrained and relaxed NT structures. We find that for the constrained structure, the band-gap increases linearly with twisting angle up to $16^\circ/\text{nm}^{-1}$, then gradually decreases to zero at higher angles. Allowing relaxation in the twisted nanotube structure has a strong influence on the value of the band-gap; the gap increases linearly (but with a different slope) with twisting angle up to $14^\circ/\text{nm}^{-1}$, then reaches a stable value (≈ 0.3 eV) at higher angles. The first, linear, region corresponds to the opening of a gap produced by the strong effects of symmetry breaking on the frontier π and π^* orbitals. This initial linear increase obtained in constrained structures is in general agreement with the predictions of low energy theory [8] which, however, does not take relaxation into account. For higher twisting angles, the band-gap decrease observed for the constrained geometry is mainly due to the presence of highly destabilized $\sigma - \sigma^*$ -orbitals near the Fermi level that emerge from the increasing $(sp)_\sigma - (sp)_\sigma$ overlap. The plateau observed in relaxed structures is the result of the collapse of the tubular structure into a flattened helix shape which decreases the large repulsive overlap of strained NTs (Fig.2c,d).

The opening of a band-gap in originally metallic nan-

otubes leads to a drastic modification of the electrical properties of nanotubes upon twisting by even low angles. In order to investigate the conduction of electrons in twisted (and relaxed) (6,6) nanotubes, we have connected both tube ends (with dangling bonds on the end carbons) to gold electrodes. Each electrode is composed of a layer of 22 gold atoms in a (111) crystalline arrangement. The distance between the NT end and the gold layer is 1.0 \AA . Such a bonding configuration minimizes the contact-resistance and emphasizes the transport properties of the nanotube itself. The Hamiltonian (H_{NT}) and overlap matrices (S_{NT}) of equation (1) are determined using EHM for the system Gold-NT-Gold. The transmission function $T(E)$, that represents the sum of the transmission probabilities over the contributing nanotube conduction channels, is then computed from equation (3). The $T(E)$ spectra are expressed with respect to the Fermi level (E_F is defined as 0 eV) of individual twisted nanotubes.

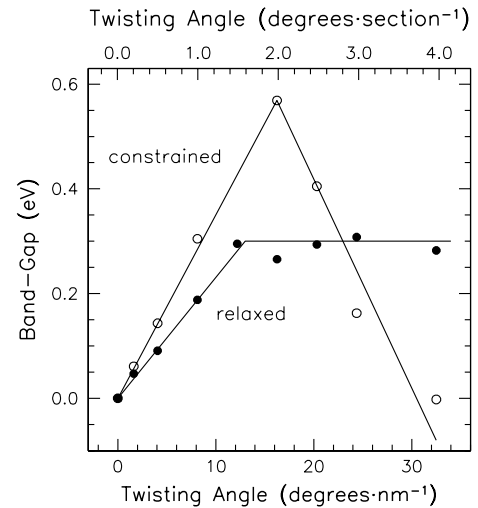


FIG. 3. Band-gap opening in a (6,6) nanotube as a function of the twist angle for a constrained geometry (open circles), and a relaxed geometry (closed circles).

Figure 4 shows the transmission $T(E)$ spectra of nanotubes twisted by $0, 1.6, 4.1$ and $8.1^\circ/\text{nm}^{-1}$ angles (main panel). All these deformed tubes lie within the linear regime of the band-gap variation with twist angle. The variation of $T(E)$ at E_F with twisting angle is shown at the upper-left panel, while the corresponding change in resistance at zero bias ($= 12.9 \text{ k}\Omega/T(E_F)$) is given at the upper-right panel. The spectrum of the perfect structure ($0^\circ/\text{nm}^{-1}$) shows a $T(E)$ at the Fermi level of about 1.2, leading to a resistance higher than expected for ballistic transport (where $T(E) = 2.0$). This reduction in transmission is due to the presence of a finite contact resistance. The increasing $T(E)$ on the high binding energy side is due to the opening of higher conduction channels. The asymmetry of the transmission function $T(E)$ above and below E_F depends on the NT-metal electrode cou-

pling (Au-NT distance). A larger Au-NT distance leads to a higher $T(E)$ above E_F , and vice versa. Since the NT-metal electrode distance is kept fixed in all calculations, this effect of contact resistance does not influence the effects induced by tube twisting.

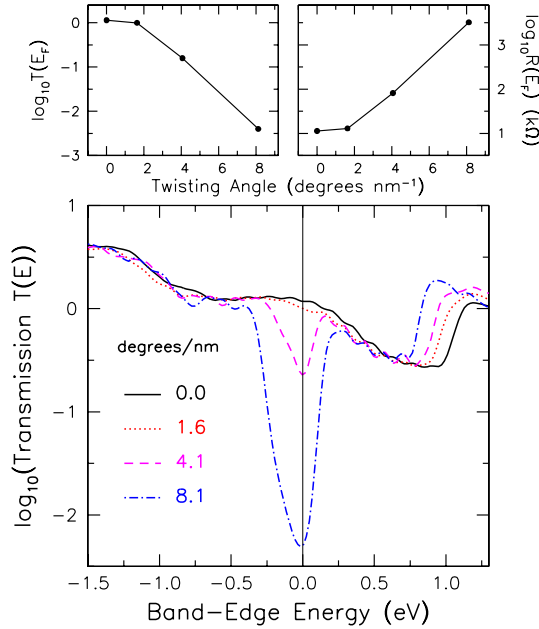


FIG. 4. Computed transmission function of a twisted (6,6) NT. The upper-left inset shows the logarithmic decay of $T(E_F)$ with twisting angle, and the upper-right inset gives the variation of the resistance at zero bias for the same twisted NT.

Twisting induces important changes in the $T(E_F)$, a property that determines the linear conductance of the system. Already a twist of 4° nm^{-1} (or $0.5^\circ \text{ section}^{-1}$), reduces the transmission by a factor of 14. It is interesting, however, that essentially no change is seen in $T(E_F)$ at low twisting angles ($< 2^\circ \text{ nm}^{-1}$) despite the fact that a finite band-gap ($\approx 0.04 \text{ eV}$) is calculated for the free NT. We attribute this behavior to the metal-induced gap states (MIGS) produced by the interaction of the short (96 \AA) NT segment with the gold metal electrodes [21] and the presence of charge-transfer doping. The MIGS tend to bridge the distortion-induced gap when the latter is small [22]. For twisting angles larger than 2° nm^{-1} , the transmission decreases exponentially (see upper-left in Fig. 4). At 8° nm^{-1} , $T(E_F)$ has been decreased by more than 2 orders of magnitude, and if we consider transport into a strongly twisted, helical shape nanotube (see Fig.2 [c,d]), the decrease in $T(E)$ is about 5 orders of magnitude. A twisting-induced band-gap is, most likely, responsible for the recently documented field-effect transistor action of a twisted, normally metallic multi-wall nanotube [3].

In contrast to our findings on axially bent nanotubes [13] where for a (6,6) tube the decrease in transmis-

sion occurred at energies below E_F , and was traced to curvature-induced localized σ - π orbital mixing, the sharp decrease in $T(E)$ upon twisting straddles E_F and is induced by symmetry breaking all along the NT.

We thank Dr. Thomas Heine for providing us the tight-binding DFT code, and Dr. Frédéric Lesage for very helpful discussions.

-
- [1] S.J. Tans, A.R.M. Verschueren, and C. Dekker, *Nature* **393**, 49 (1998).
 - [2] M. Bockrath, D.H. Cobden, P.L. McEuen, N.G. Chopra, A. Zettl, A. Thess, and R. E. Smalley *Science* **275**, 1922 (1997).
 - [3] R. Martel, T. Schmidt, H.R. Shea, T. Hertel, and Ph. Avouris, *Appl. Phys. Lett.* **73**, 2447 (1998).
 - [4] M.S. Dresselhaus, G. Dresselhaus, and P.C. Eklund, *Science of Fullerenes and Carbon Nanotubes* (Academic, San Diego, 1996).
 - [5] T. Hertel, R.E. Walkup, and Ph. Avouris, *Phys. Rev. B* **58**, 13870 (1998).
 - [6] W. Clauss, D.J. Bergeron, and A.T. Johnson, *Phys. Rev. B* **58**, 4266 (1998).
 - [7] N.G. Chopra, et al., *Nature* **377**, 135 (1995).
 - [8] C.L. Kane, and E.J. Mele, *Phys. Rev. Lett.* **78**, 1932 (1997).
 - [9] C.L. Kane, E.J. Mele, R.S. Lee, J.E. Fischer, P. Petit, H. Dai, A. Thess, R.E. Smalley, A.R.M. Verschueren, S.J. Tans, and C. Dekker, *Europhys. Lett.* **41**, 683 (1998).
 - [10] N. Hamada, S. Sawada, and A. Oshiyama, *Phys. Rev. Lett.* **68**, 1579 (1992).
 - [11] J.W. Mintmire, B.I. Dunlap, and C.T. White, *Phys. Rev. Lett.* **68**, 631 (1992).
 - [12] R. Saito, M. Fujita, G. Dresselhaus, and M. Dresselhaus, *Appl. Phys. Lett.*, **60**, 2204 (1992).
 - [13] A. Rochefort, F. Lesage, D.R. Salahub, and Ph. Avouris, submitted to *Phys. Rev. B*.
 - [14] Y. Kong, and J.W. Ponder, *J. Chem. Phys.* **107**, 481 (1997).
 - [15] A. Rochefort, D.R. Salahub, and Ph. Avouris, *Chem. Phys. Lett.* **297**, (1998) 45.
 - [16] D. Porezag, Th. Frauenheim, Th. Köhler, G. Seifert, and R. Kaschner, *Phys. Rev. B* **51**, 12947 (1995).
 - [17] Landrum, G. *YAEHMOP* (Yet Another Extended Hückel Molecular Orbital Package), Cornell University, Ithaca, NY, 1995.
 - [18] A. Rochefort, D.R. Salahub, and Ph. Avouris, *J. Phys. Chem.* **103**, (1999) 641.
 - [19] S. Datta, *Electronic Transport in Mesoscopic Systems*, (Cambridge University Press, Cambridge, U.K., 1995).
 - [20] B.I. Yakobson, C.J. Brabec, and J. Bernholc, *Phys. Rev. Lett.* **76**, 2511 (1996).
 - [21] V. Heine, *Phys. Rev. A* **138**, 1689 (1965).
 - [22] F. Leonard and J. Tersoff, to be published.